Published in IET Control Theory and Applications
Received on 8th February 2012
Revised on 6th December 2012
Accepted on 7th January 2013
doi: 10.1049/iet-cta.2012.0459

ISSN 1751-8644

Overcoming passivity violations: closed-loop stability, controller design and controller scheduling

James Richard Forbes[1], *Christopher John Damaren*[2]

[1]*Department of Mechanical Engineering and Centre for Intelligent Machines, McGill University, 817 Sherbrooke Street West, Montreal, Quebec, Canada, H3A 0C3*
[2]*University of Toronto, Institute for Aerospace Studies, 4925 Dufferin Street, Toronto, Ontario, Canada, M3H 5T6*
E-mail: james.richard.forbes@mcgill.ca

Abstract: Control of systems that have had their passive input–output map partially violated is the motivation of this study. The hybrid passivity/finite-gain systems framework is specifically well suited to systems that have experienced a passivity violation. The focus of this study is the extension and application of the hybrid passivity/finite-gain systems framework to a multi-input multi-output (MIMO) control problem. Calculation of the hybrid passivity/finite-gain parameters in a linear time-invariant (LTI) MIMO context is considered. Additionally, we show that a set of hybrid very strictly passive/finite-gain (VSP/finite-gain) controllers gain-scheduled in a particular way also possesses hybrid VSP/finite-gain properties. To synthesise hybrid VSP/finite-gain controllers a frequency-weighted optimal control scheme is used to parameterise controllers that are then constrained and optimised within a numerical optimisation framework. The theoretical contributions of this work are validated experimentally using a two-link flexible manipulator apparatus. Results highlight the utility of the hybrid passivity/finite-gain framework, the scheduling scheme and controller design method.

1 Introduction

Passive systems, their stability in feedback and passivity-based control formulations are well documented [1–7]. While using a passivity-based control scheme, it is generally assumed that control inputs can be applied exactly, and plant outputs can be measured directly. In practice, desired control inputs are applied via actuators that are dynamical. Similarly, the plant outputs are generally measured by sensors that have dynamics, or estimated via a filtering technique. Actuators, sensors and filters that have unity gain and zero phase lag over all frequencies do not exist. Such dynamics generally destroy the nominally passive input–output (I–O) map to be used as the basis for robust stabilisation via the passivity theorem; in reality passivity is 'violated'.

Motivated by passivity violations, the hybrid passivity and finite-gain (hybrid passivity/finite gain) systems framework has been developed [8, 9]. The hybrid systems framework is of the I–O type, much like the traditional passivity and small-gain framework. Hybrid passivity/finite-gain systems are similar to the 'mixed' systems discussed in [10, 11], and the finite frequency positive real systems explored in [12]. In a linear time-invariant (LTI) context, hybrid passivity/finite-gain systems are those that possess a passive I–O map over a frequency band, and a finite-gain I–O map when passivity has been violated. Although it is perhaps intuitive to think in terms of a system's frequency response, the hybrid passivity/finite-gain systems framework is applicable to non-linear systems as well. For control, the negative feedback interconnection of hybrid passivity/finite-gain systems is of interest, as addressed by the hybrid passivity/finite-gain stability theorem. The hybrid passivity/finite-gain stability theorem relies on both passivity and small-gain arguments in tandem; when a passive I–O map exists stability is guaranteed via a passivity theorem type argument, and when a passivity violation occurs bounded plant and controller gains ensure destabilisation does not occur. The word hybrid is used to highlight how the passivity theorem and the small-gain theorem are used in a 'hybrid', 'mixed' or 'blended' fashion within the hybrid passivity/finite-gain systems framework; the word hybrid is not used in the sense that there is some sort of switching.

The goal of this paper is to further develop and experimentally validate the hybrid passivity/finite-gain systems framework. In particular, joint-based control of a flexible robotic manipulator is considered. Control of a flexible robotic manipulator is challenging owing to the non-linear nature of the problem, but also has performance issues associated with vibration suppression and trajectory tracking [13–17]. To explicitly motivate the use of the hybrid passivity/finite-gain systems framework, the nominally passive nature of the flexible manipulator to be controlled is discussed, as well as a simple passivity violation induced by filtering of the available measurements. With a clear motivation, paper [8] is reviewed and expanded upon. The very strictly passive (VSP) and finite-gain parameters associated with hybrid systems will be defined in an LTI, multi-input multi-output (MIMO) context. With the control of a non-linear plant in

mind, a set of hybrid VSP/finite-gain subsystems scheduled (that is to say 'gain-scheduled') in a particular fashion is shown to possesses hybrid VSP/finite-gain properties. The design of LTI MIMO controllers using a frequency-weighted optimal control parameterisation is then considered. A numerical optimisation scheme is employed to tune the controllers, so that the controllers to be scheduled satisfy hybrid VSP/finite-gain constraints. Last, hybrid VSP/finite-gain controllers optimally designed are used within the scheduling scheme discussed to control a two-link flexible manipulator. Experimental results confirm that good closed-loop tracking and vibration suppression is attained. This paper builds upon [8, 9] in many ways. First, the paper [8] does not consider the computation of the various hybrid passivity/finite-gain parameters, while paper [9] only considers computation of the various parameters in a single-input single-output (SISO) context. Second, we consider the gain-scheduling of controllers, and show that provided the controllers are scheduled in an appropriate way, I–O stability is assured. This result is not considered in [8, 9]. Third, we present a novel controller synthesis method, distinctly different than the method in [9], as well as others presented in the literature. Last, we consider the control of a non-linear system, while [9] considers the control of linear (time-invariant) systems only.

2 Flexible robotic systems

2.1 Ideal I-O model

A flexible robotic manipulator with N_r joints is described by

$$\mathbf{M}(\mathbf{q})\ddot{\mathbf{q}} + \mathbf{D}\dot{\mathbf{q}} + \mathbf{K}\mathbf{q} = \hat{\mathbf{B}}\boldsymbol{\tau} + \mathbf{f}_n(\mathbf{q}, \dot{\mathbf{q}}) \tag{1}$$

where $\mathbf{M} > 0$, $\mathbf{D} \geq 0$, and $\mathbf{K} \geq 0$ are the symmetric mass, damping, and stiffness matrices, $\mathbf{f}_n$ are the non-linear inertial forces, $\hat{\mathbf{B}} = [\mathbf{1}\,\mathbf{0}]^\top$, $\boldsymbol{\tau} = [\tau_1 \cdots \tau_{N_r}]^\top$ are the joint torques, $\mathbf{q} = [\boldsymbol{\theta}^\top\ \mathbf{q}_e^\top]^\top$, $\boldsymbol{\theta} = [\theta_1 \cdots \theta_{N_r}]^\top$ are the joint angles, and $\mathbf{q}_e$ are the elastic coordinates associated with the Rayleigh–Ritz discretisation of the flexible links.

It is well known that in the context of flexible mechanical systems, collocated force/torque actuators and velocity/angular velocity rate sensor yield a passive I–O map [16, 18]. In particular, the map $\boldsymbol{\tau} \to \dot{\boldsymbol{\theta}}$ associated with flexible robotic manipulators is a passive one. The map remains passive regardless of the assumed modes or discretisation method, mass distribution, etc. To robustly stabilise via the passivity theorem, an appropriate control law would be of the following form (see [16], section 4.4.3; [19, 20])

$$\boldsymbol{\tau}(s) = \boldsymbol{\tau}_{\text{ff}}(s) - \left[\frac{1}{s}\mathbf{K}_{\text{p}} + \mathbf{G}_{\text{VSP}}(s)\right]\dot{\boldsymbol{\theta}}(s) \tag{2}$$

where $\boldsymbol{\tau}_{\text{ff}}$ is a feedforward control that effectively negates a portion of the non-linear manipulator dynamics, $\mathbf{K}_{\text{p}} = \mathbf{K}_{\text{p}}^\top > 0$ realises proportional control (note, $\frac{1}{s}\mathbf{K}_{\text{p}}$ is passive), and $\mathbf{G}_{\text{VSP}}(s)$ is a VSP transfer matrix. This control ensures that robust I–O stability of the closed-loop system in the presence of disturbances. In instances where $\dot{\boldsymbol{\theta}}$ can be directly measured, such a control law may be employed. In practice, however, $\dot{\boldsymbol{\theta}}$ is not directly measured, but estimated by filtering or finite differencing of $\boldsymbol{\theta}$ measurements.

2.2 Violation of passivity

In many practical situations $\boldsymbol{\theta}$ will be measured directly, but $\dot{\boldsymbol{\theta}}$ will not be. With $\boldsymbol{\theta}$ directly available, proportional control may be implemented without difficulty, and the result (i.e. the flexible system compensated by proportional control) is a passive plant with no rigid-body modes.

For rate control to be implemented $\dot{\boldsymbol{\theta}}$ must be estimated. A simple method to estimate $\dot{\boldsymbol{\theta}}$ is by filtering $\boldsymbol{\theta}$ as follows:

$$\mathbf{y}(s) = \mathbf{F}(s)\boldsymbol{\theta}(s) = \operatorname*{diag}_{i=1\cdots N_r}\{f(s)\}\boldsymbol{\theta}(s),$$
$$f(s) = \frac{\omega_f^2 s}{s^2 + 2\zeta_f\omega_f s + \omega_f^2} \tag{3}$$

where ω_f and ζ_f are the natural frequency and damping ratio of the derivative filter $f(s)$. Although the flexible manipulator to be controlled is non-linear, to facilitate a simpler discussion, the system's frequency response will be referred to. At low frequency $\mathbf{F}(s)$ accurately approximates $\dot{\boldsymbol{\theta}}$ and as a result the I–O map $\boldsymbol{\tau} \to \mathbf{y}$ behaves as if $\dot{\boldsymbol{\theta}}$ were measured directly, that is, passively. At higher frequencies, however, $\mathbf{F}(s)$ induces phase lag in the measurement signal to be used for control. As a result, what is fed back to the controller does not represent $\dot{\boldsymbol{\theta}}$ closely, and the I–O map $\boldsymbol{\tau} \to \mathbf{y}$ does not behave passively; passivity has been violated above a certain frequency. The true I–O map $\boldsymbol{\tau} \to \mathbf{y}$ can effectively be divided into two parts: a low-frequency part where the I–O map possesses passive characteristics, and a high-frequency part where passivity is violated. Although passivity has been violated at high frequency, the I–O map maintains finite-gain characteristics owing to the small amount of natural damping in the structure, and the natural roll-off of $\mathbf{F}(s)$. The system is hybrid, possessing both passive and finite-gain properties. Violation of passivity is this paper's motivation, and in particular the motivation behind the hybrid passivity/finite-gain stability theorem originally presented in [8].

3 Hybrid passive/finite-gain systems theory

In this section, the hybrid passive/finite-gain systems framework will be first reviewed, and then built upon [8]. Key notions are as follows: $\mathbf{y} \in L_2$ if $\|\mathbf{y}\|_2 = \langle \mathbf{y}, \mathbf{y}\rangle^{\frac{1}{2}} = \sqrt{\int_0^\infty \mathbf{y}^\top(t)\mathbf{y}\,\mathrm{d}t} < \infty$, and $\mathbf{y} \in L_{2e}$ if $\|\mathbf{y}\|_{2T} = \sqrt{\int_0^\infty \mathbf{y}_T^\top(t)\mathbf{y}_T(t)\,\mathrm{d}t} < \infty$, $0 \leq T < \infty$ where $\mathbf{y}_T(t) = \mathbf{y}(t)$, $0 \leq t \leq T$ and $\mathbf{y}_T(t) = \mathbf{0}$, $t > T$ [21].

The dissipative systems framework of [22] is similar to the hybrid passive/finite-gain systems framework. Consider an $m \times m$ MIMO system $\mathbf{y}(t) = (\mathcal{G}\mathbf{e})(t)$, where the operator $\mathcal{G}: L_{2e} \to L_{2e}$ maps $\mathbf{e} \in L_{2e}$ to $\mathbf{y} \in L_{2e}$. A hybrid passive/finite-gain system is one which satisfies [8]

$$\langle \mathbf{y}_T, \mathcal{Q}\mathbf{y}_T\rangle + 2\langle \mathbf{y}_T, \mathcal{S}\mathbf{e}_T\rangle + \langle \mathbf{e}_T, \mathcal{R}\mathbf{e}_T\rangle \geq 0 \tag{4}$$

where

$$\mathcal{Q} = -[\epsilon\tilde{\mathcal{A}}\mathcal{A} + \gamma^{-1}\tilde{\mathcal{B}}\mathcal{B}],$$
$$\mathcal{S} = \frac{1}{2}\tilde{\mathcal{A}}\mathcal{A}, \tag{5}$$
$$\mathcal{R} = [\gamma\tilde{\mathcal{B}}\mathcal{B} - \delta\tilde{\mathcal{A}}\mathcal{A}]$$

doi: 10.1049/iet-cta.2012.0459

are operators. The constants δ, ε, and γ are non-negative, and the operators $\boldsymbol{\mathcal{A}}$ and $\boldsymbol{\mathcal{B}}$ are defined as follows

$$\begin{aligned}&\boldsymbol{\mathcal{A}}^{\sim}\boldsymbol{\mathcal{A}}+\boldsymbol{\mathcal{B}}^{\sim}\boldsymbol{\mathcal{B}}=\boldsymbol{1}\\&\Leftrightarrow \underbrace{\mathbf{A}^{\top}(-j\omega)\mathbf{A}(j\omega)}_{\alpha(\omega)\mathbf{1}}+\underbrace{\mathbf{B}^{\top}(-j\omega)\mathbf{B}(j\omega)}_{\beta(\omega)\mathbf{1}}=\mathbf{1}\\&\Leftrightarrow \alpha(\omega)+\beta(\omega)=1\end{aligned}\tag{6}$$

where $\boldsymbol{1}$ is the $m\times m$ identity operator, $\mathbf{1}$ is the $m\times m$ identity matrix, and the transfer matrices (and functions) $\mathbf{A}(s)=A(s)\mathbf{1}$ and $\mathbf{B}(s)=B(s)\mathbf{1}$ are causal with time-domain equivalent operators $\boldsymbol{\mathcal{A}}{:}L_2\to L_2$ and $\boldsymbol{\mathcal{B}}{:}L_2\to L_2$. The operator adjoints of $\boldsymbol{\mathcal{A}}$ and $\boldsymbol{\mathcal{B}}$ are $\boldsymbol{\mathcal{A}}^{\sim}$ and $\boldsymbol{\mathcal{B}}^{\sim}$. The frequency-dependent functions $\alpha{:}\mathbb{R}\to\{0,1\}$ and $\beta{:}\mathbb{R}\to\{0,1\}$ are theoretical abstractions used to distinguish between passive system characteristics and non-passive but still finite-gain system characteristics. When the system in question possesses a passive I–O map, $\alpha(\omega)=1$ and $\beta(\omega)=0$. When the system fails to possess a passive I–O map, that is the system has experienced a passivity violation, but the map has finite gain, $\alpha(\omega)=0$ and $\beta(\omega)=1$. The divide occurs at a critical frequency, ω_{c}, which is used to define α and β

$$\begin{aligned}\alpha(\omega)&=\left.\begin{cases}1, & -\omega_{\mathrm{c}}<\omega<\omega_{\mathrm{c}}, \quad \text{(passive region)}\\ 0, & |\omega|\geq\omega_{\mathrm{c}}, \quad \text{(finite-gain region)}\end{cases}\right\}\\&=A(-j\omega)A(j\omega)=|A(j\omega)|^2\end{aligned}\tag{7}$$

$$\begin{aligned}\beta(\omega)&=\left.\begin{cases}0, & -\omega_{\mathrm{c}}<\omega<\omega_{\mathrm{c}}, \quad \text{(passive region)}\\ 1, & |\omega|\geq\omega_{\mathrm{c}}, \quad \text{(finite-gain region)}\end{cases}\right\}\\&=B(-j\omega)B(j\omega)=|B(j\omega)|^2\end{aligned}\tag{8}$$

The functions α and β can intuitively be thought of as ideal low-pass and high-pass filters that filter the I–O signals into two parts: a passive part and a finite-gain part.

Using (5), (4) can be written as

$$\begin{aligned}&\langle\boldsymbol{\mathcal{A}}\mathbf{y}_T,\boldsymbol{\mathcal{A}}\mathbf{e}_T\rangle-\delta\langle\boldsymbol{\mathcal{A}}\mathbf{e}_T,\boldsymbol{\mathcal{A}}\mathbf{e}_T\rangle-\epsilon\langle\boldsymbol{\mathcal{A}}\mathbf{y}_T,\boldsymbol{\mathcal{A}}\mathbf{y}_T\rangle+\gamma\langle\boldsymbol{\mathcal{B}}\mathbf{e}_T,\boldsymbol{\mathcal{B}}\mathbf{e}_T\rangle\\&\quad-\gamma^{-1}\langle\boldsymbol{\mathcal{B}}\mathbf{y}_T,\boldsymbol{\mathcal{B}}\mathbf{y}_T\rangle\geq 0\end{aligned}$$

Alternatively, (4) can be written in the frequency domain via Parseval's theorem

$$\begin{aligned}&\frac{1}{2\pi}\int_{-\infty}^{\infty}\mathbf{y}_T^{\top}(-j\omega)\mathbf{Q}(\omega)\mathbf{y}_T(j\omega)\,\mathrm{d}\omega\\&\quad+\frac{1}{\pi}\mathrm{Re}\int_{-\infty}^{\infty}\mathbf{y}_T^{\top}(-j\omega)\mathbf{S}(\omega)\mathbf{e}_T(j\omega)\,\mathrm{d}\omega\\&\quad+\frac{1}{2\pi}\int_{-\infty}^{\infty}\mathbf{e}_T^{\top}(-j\omega)\mathbf{R}(\omega)\mathbf{e}_T(j\omega)\,\mathrm{d}\omega\geq 0\end{aligned}\tag{9}$$

where $\mathrm{Re}\{\cdot\}$ is the real part of the argument. By using (6), we have

$$\begin{aligned}&\mathbf{Q}(\omega)=-[\epsilon\alpha(\omega)+\gamma^{-1}\beta(\omega)]\mathbf{1},\quad \mathbf{S}(\omega)=\frac{1}{2}\alpha(\omega)\mathbf{1},\\&\mathbf{R}(\omega)=[\gamma\beta(\omega)-\delta\alpha(\omega)]\mathbf{1}.\end{aligned}\tag{10}$$

The constants δ and ϵ depend on the passive nature of the system, and γ depends on the finite-gain nature of the system when passivity is violated. Note in (10) that the units of $\mathbf{Q}(\omega)$ and $\mathbf{R}(\omega)$ are consistent: ϵ and γ^{-1} have units of one over gain, whereas δ and γ have units of gain. Sufficient conditions for (9) to hold are

$$\begin{aligned}\frac{1}{2\pi}\mathrm{Re}\int_{-\omega_{\mathrm{c}}}^{\omega_{\mathrm{c}}}\mathbf{y}_T^{\top}(-j\omega)\mathbf{e}_T(j\omega)\,\mathrm{d}\omega&\geq\frac{\delta}{2\pi}\int_{-\omega_{\mathrm{c}}}^{\omega_{\mathrm{c}}}\mathbf{e}_T^{\top}(-j\omega)\mathbf{e}_T(j\omega)\,\mathrm{d}\omega\\&+\frac{\epsilon}{2\pi}\int_{-\omega_{\mathrm{c}}}^{\omega_{\mathrm{c}}}\mathbf{y}_T^{\top}(-j\omega)\mathbf{y}_T(j\omega)\,\mathrm{d}\omega\end{aligned}\tag{11}$$

and

$$\begin{aligned}&\frac{1}{\gamma\pi}\int_{\omega_{\mathrm{c}}}^{\infty}\mathbf{y}_T^{\top}(-j\omega)\mathbf{y}_T(j\omega)\,\mathrm{d}\omega\\&\quad\leq\frac{\gamma}{\pi}\int_{\omega_{\mathrm{c}}}^{\infty}\mathbf{e}_T^{\top}(-j\omega)\mathbf{e}_T(j\omega)\,\mathrm{d}\omega\end{aligned}\tag{12}$$

which is to say adding (11) and (12) gives (9). When $\alpha(\omega)=1$ (and $\beta(\omega)=0$) in (9) the I–O map is said to be

1. Passive if $\delta=\epsilon=0$,
2. VSP or input strictly passive (ISP) with finite-gain if $\delta>0$ and $\epsilon>0$,
3. ISP if $\delta>0$ and $\epsilon=0$, and
4. Output strictly passive (OSP) if $\delta=0$ and $\epsilon>0$.

If a passive I–O map no longer exists, that is passivity has been violated, $\alpha(\omega)=0$ (and $\beta(\omega)=1$) then the I–O map in (9) is said to be a finite-gain I–O map.

It is worth noting that the I–O signals of the system in question, $\mathbf{e}$ and $\mathbf{y}$, are Fourier transformed, but the system operator $\boldsymbol{\mathcal{G}}{:}L_{2e}\to L_{2e}$ is not. The hybrid passivity/finite-gain systems framework holds for both linear and non-linear systems, although it is perhaps more intuitive to envision the hybrid character of a plant in terms of a frequency response, which is a linear concept. Additionally, note that if a passivity violation does not occur, that is the system is passive over all frequencies, $\omega_{\mathrm{c}}\to\infty$ and from (4) and (5) (or (9) and (10)) the traditional passivity inequality is recovered. Similarly, if a system is not passive but does have finite gain, $\omega_{\mathrm{c}}=0$ and from (4) and (5) (or (9) and (10)) the traditional finite-gain inequality is recovered.

Next the hybrid passivity/finite-gain stability theorem will be presented [8]. Consider the negative feedback interconnection of two hybrid passivity/finite-gain systems, $\boldsymbol{\mathcal{G}}_1$ and $\boldsymbol{\mathcal{G}}_2$, presented in Fig. 1.The passivity and finite-gain parameters for each system are δ_1, ϵ_1, and γ_1 and δ_2, ϵ_2, and γ_2, respectively.

Theorem 3.1: Given $\boldsymbol{\mathcal{G}}_1{:}L_{2e}\to L_{2e}$ and $\boldsymbol{\mathcal{G}}_2{:}L_{2e}\to L_{2e}$, the negative feedback interconnection presented in Fig. 1 is L_2-stable if the variables δ_1, ϵ_1, γ_1, δ_2, ϵ_2 and γ_2 satisfy $\epsilon_1+\delta_2>0$, $\epsilon_2+\delta_1>0$ and $\gamma_1\gamma_2<1$.

Proof: See Theorem 2 and Corollary 1 in [8].

The hybrid passivity/finite-gain stability theorem is an amalgamation of the traditional passivity and small-gain theorems. Its creation and development is motivated by systems that are nominally passive, but have had their passive

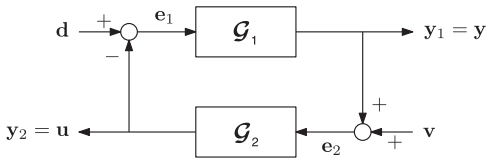

Fig. 1 *General negative feedback interconnection of systems* $\mathcal{G}_1$ *and* $\mathcal{G}_2$

I–O map partially destroyed in some way. The hybrid passivity/finite-gain stability theorem allows high-gain feedback to be partially reintroduced where the traditional small-gain theorem would be overly conservative and the traditional passivity theorem alone would not guarantee closed-loop stability at all. Note that L_2-stability is assured (like the traditional passivity and small-gain theorems), meaning that provided the inequalities $\epsilon_1 + \delta_2 > 0$, $\epsilon_2 + \delta_1 > 0$ and $\gamma_1\gamma_2 < 1$ are satisfied and $\mathbf{d}, \mathbf{v} \in L_2$, then $\mathbf{y}, \mathbf{u} \in L_2$.

In order to use the hybrid passivity/finite-gain stability theorem, the hybrid passivity/finite-gain parameters δ, ϵ and γ must be quantified. Given a general MIMO system $\mathbf{y}(t) = (\mathcal{G}\mathbf{e})(t)$, possibly non-linear, the passivity/finite-gain parameters can be approximated using the linearised system, $\mathbf{y}(s) = \mathbf{G}(s)\mathbf{e}(s)$, where $\mathbf{G}(s)$ is the system transfer matrix. If the original system is LTI, then $\mathbf{G}(s)$ exactly represents the original system, whereas if the system is non-linear, $\mathbf{G}(s)$ represents the linearised system.

Hybrid ISP system properties will be considered first. To see how the ISP parameter δ can be computed, consider manipulation of the following inner product

$$\begin{aligned}
&\frac{1}{2\pi}\mathrm{Re}\int_{-\omega_c}^{\omega_c} \mathbf{y}_T^{\top}(-j\omega)\mathbf{e}_T(j\omega)\,\mathrm{d}\omega \\
&\quad = \frac{1}{4\pi}\int_{-\omega_c}^{\omega_c} \mathbf{e}_T^{\top}(-j\omega)[\mathbf{G}^{\top}(-j\omega) + \mathbf{G}(j\omega)]\mathbf{e}_T(j\omega)\,\mathrm{d}\omega \\
&\quad \geq \underbrace{\frac{1}{2}\inf_{-\omega_c<\omega<\omega_c} \underline{\lambda}\{\mathbf{G}^{\top}(-j\omega) + \mathbf{G}(j\omega)\}}_{\delta} \\
&\qquad \frac{1}{2\pi}\int_{-\omega_c}^{\omega_c} \mathbf{e}_T^{\top}(-j\omega)\mathbf{e}_T(j\omega)\,\mathrm{d}\omega
\end{aligned} \tag{13}$$

where $\delta = \frac{1}{2}\inf_{-\omega_c<\omega<\omega_c} \underline{\lambda}\{\mathbf{G}^{\top}(-j\omega) + \mathbf{G}(j\omega)\}$ and $\underline{\lambda}\{\cdot\}$ is the minimum eigenvalue.

Next hybrid VSP system characteristics will be considered, and in particular the calculation of the OSP parameter ϵ. Recall that a VSP system is also an ISP system that possess finite gain. The so-called passive system gain can be calculated as follows

$$\begin{aligned}
&\frac{1}{2\pi}\int_{-\omega_c}^{\omega_c} \mathbf{y}_T^{\top}(-j\omega)\mathbf{y}_T(j\omega)\,\mathrm{d}\omega \\
&\quad = \frac{1}{2\pi}\int_{-\omega_c}^{\omega_c} \mathbf{e}_T^{\top}(-j\omega)\mathbf{G}^{\top}(-j\omega)\mathbf{G}(j\omega)\mathbf{e}_T(j\omega)\,\mathrm{d}\omega \\
&\quad \leq \underbrace{\sup_{-\omega_c<\omega<\omega_c} \bar{\sigma}^2\{\mathbf{G}(j\omega)\}}_{\kappa^2} \frac{1}{2\pi}\int_{-\omega_c}^{\omega_c} \mathbf{e}_T^{\top}(-j\omega)\mathbf{e}_T(j\omega)\,\mathrm{d}\omega
\end{aligned} \tag{14}$$

where $\bar{\sigma}\{\cdot\}$ is the maximum singular value. Therefore $\kappa = \sup_{-\omega_c<\omega<\omega_c} \bar{\sigma}\{\mathbf{G}(j\omega)\}$ and is referred to as the passive system gain. To show that a hybrid ISP, finite-gain system is hybrid VSP, start with the hybrid ISP inequality presented in (13), let $\bar{\delta} = \delta/2$, and substitute (14) as follows [21]

$$\begin{aligned}
&\frac{1}{2\pi}\mathrm{Re}\int_{-\omega_c}^{\omega_c} \mathbf{y}_T^{\top}(-j\omega)\mathbf{e}_T(j\omega)\,\mathrm{d}\omega \\
&\quad \geq \frac{\bar{\delta}}{2\pi}\int_{-\omega_c}^{\omega_c} \mathbf{e}_T^{\top}(-j\omega)\mathbf{e}_T(j\omega)\,\mathrm{d}\omega \\
&\qquad + \frac{\bar{\delta}}{2\pi}\int_{-\omega_c}^{\omega_c} \mathbf{e}_T^{\top}(-j\omega)\mathbf{e}_T(j\omega)\,\mathrm{d}\omega \\
&\quad \geq \frac{\bar{\delta}}{2\pi}\int_{-\omega_c}^{\omega_c} \mathbf{e}_T^{\top}(-j\omega)\mathbf{e}_T(j\omega)\,\mathrm{d}\omega \\
&\qquad + \underbrace{\frac{\bar{\delta}}{\kappa^2}}_{\bar{\epsilon}} \frac{1}{2\pi}\int_{-\omega_c}^{\omega_c} \mathbf{y}_T^{\top}(-j\omega)\mathbf{y}_T(j\omega)\,\mathrm{d}\omega
\end{aligned} \tag{15}$$

Hence, a hybrid ISP, finite-gain system is clearly hybrid VSP where the OSP parameter is $\bar{\delta}/\kappa^2$. Therefore stating a hybrid system has $\delta > 0$ and $\kappa < \infty$ implies $\delta > 0$ and $\epsilon > 0$.

Finally, the finite-gain parameter associated with an I–O map that is no longer passive can be calculated as follows

$$\begin{aligned}
&\frac{1}{\pi}\int_{\omega_c}^{\infty} \mathbf{y}_T^{\top}(-j\omega)\mathbf{y}_T(j\omega)\,\mathrm{d}\omega \\
&\quad \leq \underbrace{\sup_{\omega\geq\omega_c} \bar{\sigma}^2\{\mathbf{G}(j\omega)\}}_{\gamma^2} \frac{1}{\pi}\int_{\omega_c}^{\infty} \mathbf{e}_T^{\top}(-j\omega)\mathbf{e}_T(j\omega)\,\mathrm{d}\omega
\end{aligned} \tag{16}$$

Thus, $\gamma = \sup_{\omega\geq\omega_c} \bar{\sigma}\{\mathbf{G}(j\omega)\}$.

4 Scheduling of hybrid VSP/finite-gain systems

We will show that N hybrid VSP/finite-gain subsystems of the form $\mathbf{y}_i = (\mathcal{G}_i\mathbf{e}_i)(t)$ (where $\delta_i > 0$, $\kappa_i < \infty$ and $\gamma_i < \infty$) 'gain-scheduled' in an appropriate fashion yields a hybrid VSP/finite-gain system.To start, recall from (6) that $\mathcal{I} = \mathcal{A}^{\sim}\mathcal{A} + \mathcal{B}^{\sim}\mathcal{B}$ where $\mathcal{I}$ is the identity operator.Using this relationship, a function, such as $\mathbf{y}$, may be written as

$$\mathbf{y}(t) = (\mathcal{I}\mathbf{y})(t) = (\mathcal{A}^{\sim}\mathcal{A}\mathbf{y})(t) + (\mathcal{B}^{\sim}\mathcal{B}\mathbf{y})(t) \tag{17}$$

Next consider the scheduling architecture of Fig. 2 [19, 20]. The scheduling signals, s_i, are applied to both the input and output of the subsystems

$$\mathbf{y}(t) = \sum_{i=1}^{N} s_i(t)\mathbf{y}_i(t), \qquad \mathbf{e}_i(t) = s_i(t)\mathbf{e}(t) \tag{18}$$

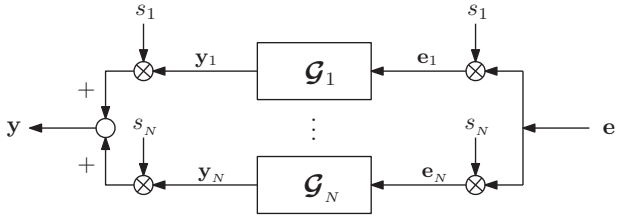

Fig. 2 *Scheduling architecture where the* $\otimes$ *symbol indicates multiplication (i.e.* $\mathbf{e}_i(t) = s_i(t)\mathbf{e}(t)$*)*

doi: 10.1049/iet-cta.2012.0459

The signals satisfy $\sum_{i=1}^{N} s_i^2(t) \geq \nu > 0$ (i.e. one scheduling signal must be active at all times), and $s_i \in L_{2e} \cap L_\infty$. Using (17), (18) can be written as

$$\begin{aligned}\mathbf{y}(t) &= \sum_{i=1}^{N} s_i(t)\mathbf{y}_i(t) \\ &= \sum_{i=1}^{N} s_i(t)\big((\mathcal{A}\tilde{\mathcal{A}}\mathbf{y}_i)(t) + (\mathcal{B}\tilde{\mathcal{B}}\mathbf{y}_i)(t)\big) \qquad (19a)\end{aligned}$$

$$\mathbf{e}_i(t) = s_i(t)\mathbf{e}(t) = s_i(t)\big((\mathcal{A}\tilde{\mathcal{A}}\mathbf{e})(t) + (\mathcal{B}\tilde{\mathcal{B}}\mathbf{e})(t)\big) \qquad (19b)$$

In this paper, we will assume the scheduling signals are a function of time only, but they could be a function of another variable

Theorem 4.1: The map $\mathbf{e} \to \mathbf{y}$ of Fig. 2 is hybrid VSP/finite gain with $\delta > 0$, $0 < \kappa < \infty$, and $0 < \gamma < \infty$, if each of the subsystems $\mathbf{y}_i = (\mathcal{G}_i\mathbf{e}_i)(t)$ is hybrid VSP/finite gain with $\delta_i > 0$, $0 < \kappa_i < \infty$ and $0 < \gamma_i < \infty$, and are scheduled via (19).

Proof: Proof of Theorem 4.1 will be executed in two steps: first it will be shown that a set of subsystems that are ISP when passivity holds and are scheduled via the architecture of Fig. 2 yields an overall gain-scheduled system that is also ISP when passivity holds. Then it will be shown that provided each hybrid VSP/finite-gain subsystem possesses finite gain in both the passive and non-passive bands, the overall gain-scheduled system possess finite gain in the passive and non-passive bands as well (although the gain in the passive and non-passive bands may be different). Combining the ISP and finite-gain nature when passivity holds, plus the finite-gain nature when passivity is violated, proves that the scheduled system is a hybrid VSP/finite-gain system.

The ISP property when passivity holds will be considered first. To begin, note that

$$\begin{aligned}&\int_0^\infty (\mathcal{A}\tilde{\mathcal{A}}\mathbf{e}_T)^\top(t)(\mathcal{B}\tilde{\mathcal{B}}\mathbf{y}_T)(t)\,\mathrm{d}t \\ &= \frac{1}{2\pi}\int_{-\infty}^{\infty} \mathbf{e}_T^\top(-j\omega)\underbrace{\mathbf{A}^\top(-j\omega)\mathbf{A}(j\omega)}_{\mathbf{1}\alpha(\omega)}\underbrace{\mathbf{B}^\top(-j\omega)\mathbf{B}(j\omega)}_{\mathbf{1}\beta(\omega)}\mathbf{y}_T(j\omega)\,\mathrm{d}\omega \\ &= 0 \qquad (20)\end{aligned}$$

owing to the fact that the product $\alpha(\omega)\beta(\omega)$ is zero (refer to the definition of α and β in (7) and (8) of Section 3). Now, consider the following integral and subsequent manipulation

$$\begin{aligned}&\int_0^\infty (\mathcal{A}\mathbf{e}_T)^\top(t)(\mathcal{A}\mathbf{y}_T)(t)\,\mathrm{d}t \\ &= \int_0^\infty (\mathcal{A}\tilde{\mathcal{A}}\mathbf{e}_T)^\top(t)\mathbf{y}_T(t)\,\mathrm{d}t \\ &= \int_0^\infty (\mathcal{A}\tilde{\mathcal{A}}\mathbf{e}_T)^\top(t)\left[\sum_{i=1}^{N} s_i(t)\left[(\mathcal{A}\tilde{\mathcal{A}}\mathbf{y}_{i,T})(t)\right.\right. \\ &\quad \left.\left. + (\mathcal{B}\tilde{\mathcal{B}}\mathbf{y}_{i,T})(t)\right]\right]\mathrm{d}t \text{ (using (19a))} \\ &= \sum_{i=1}^{N}\int_0^\infty s_i(t)(\mathcal{A}\tilde{\mathcal{A}}\mathbf{e}_T)^\top(t)(\mathcal{A}\tilde{\mathcal{A}}\mathbf{y}_{i,T})(t)\,\mathrm{d}t \\ &\quad \text{(simplified using (20))} \\ &= \sum_{i=1}^{N}\int_0^\infty s_i(t)\big[(\mathcal{A}\tilde{\mathcal{A}}\mathbf{y}_{i,T})^\top(t)(\mathcal{A}\tilde{\mathcal{A}}\mathbf{e}_T)(t) \\ &\quad + (\mathcal{A}\tilde{\mathcal{A}}\mathbf{y}_{i,T})^\top(t)(\mathcal{B}\tilde{\mathcal{B}}\mathbf{e}_T)(t)\big]\mathrm{d}t\end{aligned}$$

where zero has been added in the last line. Continuing

$$\begin{aligned}&\sum_{i=1}^{N}\int_0^\infty s_i(t)(\mathcal{A}\tilde{\mathcal{A}}\mathbf{y}_{i,T})^\top(t)\underbrace{[(\mathcal{A}\tilde{\mathcal{A}}\mathbf{e}_T)(t) + (\mathcal{B}\tilde{\mathcal{B}}\mathbf{e}_T)(t)]}_{\mathbf{e}_T(t)}\,\mathrm{d}t \\ &= \sum_{i=1}^{N}\int_0^\infty s_i(t)(\mathcal{A}\tilde{\mathcal{A}}\mathbf{y}_{i,T})^\top(t)\mathbf{e}_T(t)\,\mathrm{d}t \\ &= \sum_{i=1}^{N}\int_0^\infty (\mathcal{A}\tilde{\mathcal{A}}\mathbf{y}_{i,T})^\top(t)[s_i(t)\mathbf{e}_T(t)]\mathrm{d}t \\ &= \sum_{i=1}^{N}\int_0^\infty (\mathcal{A}\tilde{\mathcal{A}}\mathbf{y}_{i,T})^\top(t)\mathbf{e}_{i,T}(t)\,\mathrm{d}t\end{aligned}$$

where the definition of $\mathbf{e}_{i_T}$ provided in (18) has been employed. Knowing that each subsystem is ISP when passivity holds it follows that

$$\begin{aligned}&\sum_{i=1}^{N}\int_0^\infty (\mathcal{A}\mathbf{y}_{i,T})^\top(t)(\mathcal{A}\mathbf{e}_{i,T})(t)\,\mathrm{d}t \\ &\geq \sum_{i=1}^{N}\delta_i\int_0^\infty (\mathcal{A}\mathbf{e}_{i,T})^\top(t)(\mathcal{A}\mathbf{e}_{i,T})(t)\,\mathrm{d}t \\ &= \sum_{i=1}^{N}\delta_i\int_0^\infty (\mathcal{A}\tilde{\mathcal{A}}\mathbf{e}_{i,T})^\top(t)\left[s_i(t)\left[(\mathcal{A}\tilde{\mathcal{A}}\mathbf{e}_T)(t)\right.\right. \\ &\quad \left.\left. + (\mathcal{B}\tilde{\mathcal{B}}\mathbf{e}_T)(t)\right]\right]\mathrm{d}t \text{ (using (19b))} \\ &= \sum_{i=1}^{N}\delta_i\int_0^\infty s_i(t)(\mathcal{A}\tilde{\mathcal{A}}\mathbf{e}_{i,T})^\top(t)\underbrace{(\mathcal{A}\tilde{\mathcal{A}}\mathbf{e}_T)(t)}_{\mathbf{e}_T(t)-(\mathcal{B}\tilde{\mathcal{B}}\mathbf{e}_T)(t)}\,\mathrm{d}t \\ &\quad \text{(simplified using(20))} \\ &= \sum_{i=1}^{N}\delta_i\int_0^\infty s_i(t)(\mathcal{A}\tilde{\mathcal{A}}\mathbf{e}_T)^\top(t)\mathbf{e}_{i,T}(t)\,\mathrm{d}t \\ &= \sum_{i=1}^{N}\delta_i\int_0^\infty s_i^2(t)(\mathcal{A}\tilde{\mathcal{A}}\mathbf{e}_T)^\top(t)(\mathcal{A}\tilde{\mathcal{A}}\mathbf{e}_T)(t)\,\mathrm{d}t \\ &\quad \text{(using (19b) again, then simplifying)} \\ &\geq \delta\int_0^\infty (\mathcal{A}\mathbf{e}_T)^\top(t)(\mathcal{A}\mathbf{e}_T)(t)\,\mathrm{d}t\end{aligned}$$

where $\delta = \nu\min_{i=1,\ldots,N}\delta_i$. Thus, a set of hybrid subsystems that are ISP when passivity holds scheduled appropriately is also ISP when passivity holds.

Next the finite-gain nature of the scheduled subsystems in the passive band will be considered. Only an outline of the proof will be given; details are left to the reader. Using

(19a), (19b) and (20) in conjunction with the triangle inequality it can be shown that

$$\begin{aligned}\|\mathcal{A}\mathbf{y}_T\|_2 &= \left\|\sum_{i=1}^{N} s_i(\mathcal{A}^{\sim}\mathcal{A}\mathbf{y}_{i,T})\right\|_2 \leq \sum_{i=1}^{N}\|s_i(\mathcal{A}^{\sim}\mathcal{A}\mathbf{y}_{i,T})\|_2 \\ &\leq \sum_{i=1}^{N}\|s_i\|_\infty\|\mathcal{A}\mathbf{y}_{i,T}\|_2 \leq \sum_{i=1}^{N}\|s_i\|_\infty\kappa_i\|\mathcal{A}\mathbf{e}_{i,T}\|_2 \\ &\leq \underbrace{\left[\sum_{i=1}^{N}\|s_i\|_\infty^2\kappa_i\right]}_{\kappa}\|\mathcal{A}\mathbf{e}_T\|_2\end{aligned}$$

where $0 < \kappa < \infty$.

The finite-gain nature of the scheduled subsystems when passivity has been violated is shown in an identical fashion, resulting in

$$\|\mathcal{B}\mathbf{y}_T\|_2 \leq \underbrace{\left[\sum_{i=1}^{N}\|s_i\|_\infty^2\gamma_i\right]}_{\gamma}\|\mathcal{B}\mathbf{e}_T\|_2$$

where $0 < \gamma < \infty$. □

5 Hybrid controller design via frequency weighting and numerical optimisation

With the hybrid passivity/finite-gain stability theorem at hand, the optimal design of hybrid VSP/finite-gain controllers will now be considered.Similar to traditional controller design techniques, it is assumed that a general yet low fidelity plant model is available. If the plant is non-linear, it is linearised about an operating point. The plant model is said to be a 'low fidelity' because the true plant dynamics are modelled with a finite amount of accuracy, and the passivity-destroying filters, actuators, etc. are nominally ignored. Consistent with this assumption, it is assumed that the plant is nominally purely passive with very little dissipation, that is, $\delta_1 = 0$ and $\kappa_1 \simeq \infty$, a worst case (where δ_1 and κ_1 are defined in (13) and (14)). Furthermore, it is assumed that estimates of ω_c and $\gamma_1 < \infty$ are available (where γ_1 is defined in (16)), given a rough estimate of how the sensors and actuators behave. It should be stressed that ω_c and γ_1 can only be estimated because the true sensor and actuator dynamics are never truly known. All that really can be guaranteed is that above some ω_c a passive I–O map no longer exists, but the I–O map possesses finite gain owing to some natural damping inherent in the system.

Let us first review the $\mathcal{H}_2$ control framework [23]. The nominal plant to be controlled is

$$\dot{\mathbf{x}} = \mathbf{A}\mathbf{x} + \mathbf{B}_d\mathbf{d} + \mathbf{B}_u\mathbf{u} \tag{21a}$$

$$\mathbf{z} = \mathbf{C}_{zx}\mathbf{x} + \mathbf{D}_{zu}\mathbf{u} \tag{21b}$$

$$\mathbf{y} = \mathbf{C}_{yx}\mathbf{x} + \mathbf{D}_{yv}\mathbf{v} \tag{21c}$$

where $\mathbf{x} \in \mathbb{R}^n$ is the system state, $\mathbf{u} \in \mathbb{R}^{n_u}$ is the control input, $\mathbf{y} \in \mathbb{R}^{n_y}$ is the measurement, $\mathbf{z} \in \mathbb{R}^{n_z}$ is the regulated output, $\mathbf{d} \in \mathbb{R}^{n_d}$ is the disturbance, $\mathbf{v} \in \mathbb{R}^{n_v}$ is the measurement noise, and all matrices are dimensioned appropriately. It is assumed that

1. $(\mathbf{A}, \mathbf{B}_d)$ is controllable and $(\mathbf{C}_{zx}, \mathbf{A})$ is observable,
2. $(\mathbf{A}, \mathbf{B}_u)$ is controllable and $(\mathbf{C}_{yx}, \mathbf{A})$ is observable,
3. $\mathbf{D}_{zu}^{\top}\mathbf{C}_{zx} = \mathbf{0}$ and $\mathbf{D}_{zu}^{\top}\mathbf{D}_{zu} > 0$, and
4. $\mathbf{D}_{yv}\mathbf{B}_d^{\top} = \mathbf{0}$ and $\mathbf{D}_{yv}\mathbf{D}_{yv}^{\top} > 0$.

The optimal $\mathcal{H}_2$ controller is

$$\dot{\mathbf{x}}_c = \underbrace{(\mathbf{A} - \mathbf{B}_u\mathbf{K}_c - \mathbf{K}_e\mathbf{C}_{yx})}_{\mathbf{A}_c}\mathbf{x}_c + \underbrace{\mathbf{K}_e}_{\mathbf{B}_c}\mathbf{y}$$

$$-\mathbf{u} = \underbrace{\mathbf{K}_c}_{\mathbf{C}_c}\mathbf{x}_c$$

where $\mathbf{x}_c \in \mathbb{R}^n$ is the controller state, and $\mathbf{K}_c$ and $\mathbf{K}_e$ are the optimal state feedback and estimator gains.

The closed-loop system is described by

$$\begin{bmatrix}\dot{\mathbf{x}} \\ \dot{\mathbf{x}}_c\end{bmatrix} = \underbrace{\begin{bmatrix}\mathbf{A} & -\mathbf{B}_u\mathbf{C}_c \\ \mathbf{B}_c\mathbf{C}_{yx} & \mathbf{A}_c\end{bmatrix}}_{\mathbf{A}_{zw}}\begin{bmatrix}\mathbf{x} \\ \mathbf{x}_c\end{bmatrix} + \underbrace{\begin{bmatrix}\mathbf{B}_d & \mathbf{0} \\ \mathbf{0} & \mathbf{B}_c\mathbf{D}_{yv}\end{bmatrix}}_{\mathbf{B}_{zw}}\begin{bmatrix}\mathbf{d} \\ \mathbf{v}\end{bmatrix} \tag{22a}$$

$$\mathbf{z} = \underbrace{[\mathbf{C}_{zx} - \mathbf{D}_{zu}\mathbf{C}_c]}_{\mathbf{C}_{zw}}\begin{bmatrix}\mathbf{x} \\ \mathbf{x}_c\end{bmatrix}. \tag{22b}$$

or equivalently as $\mathbf{z}(s) = \mathbf{T}_{zw}(s)\mathbf{w}(s)$, where $\mathbf{w} = [\mathbf{d}^{\top}\ \mathbf{v}^{\top}]^{\top}$. The closed-loop $\mathcal{H}_2$-norm is

$$\mathcal{J} = \sqrt{\text{tr}\ \mathbf{B}_{zw}^{\top}\mathbf{P}_{zw}\mathbf{B}_{zw}} \tag{23}$$

where $\mathbf{P}_{zw}$ is the solution of $\mathbf{P}_{zw}\mathbf{A}_{zw} + \mathbf{A}_{zw}^{\top}\mathbf{P}_{zw} = -\mathbf{C}_{zw}^{\top}\mathbf{C}_{zw}$.

5.1 Frequency-weighted optimal control formulation

In contrast to the traditional $\mathcal{H}_2$ formulation (i.e. linear-quadratic Gaussian (LQG) control), frequency-weighted optimal control design is a technique that allows tuning of the controller frequency response. This design method is ideal in terms of numerical optimisation, where the optimisation algorithm can tune the controller. Using a numerical optimiser to optimally design the frequency weighted optimal controller subject to a set of constraints is one of the contributions of this paper. Before discussing controller synthesis via numerical optimisation, the frequency-weighted optimal control formulation will be reviewed, starting with the design of a state feedback gain matrix [24–27]. Consider the following cost function

$$\begin{aligned}\mathcal{J}_{rf} = \frac{1}{4\pi}\int_{-\infty}^{\infty}[&\mathbf{x}^{\top}(-j\omega)\mathbf{Q}_x(j\omega)\mathbf{x}(j\omega) \\ &+ \mathbf{u}^{\top}(-j\omega)\mathbf{R}_u(j\omega)\mathbf{u}(j\omega)]\text{d}\omega\end{aligned} \tag{24}$$

which is similar to the standard linear-quadratic regulator (LQR) cost function, but the weighting matrices $\mathbf{Q}_x(j\omega)$ and $\mathbf{R}_x(j\omega)$ are no longer static, but a function of frequency.

doi: 10.1049/iet-cta.2012.0459

The weights $\mathbf{Q}_x(j\omega)$ and $\mathbf{R}_u(j\omega)$ can be parameterised in terms of filters $\mathbf{W}_x(j\omega)$ and $\mathbf{W}_u(j\omega)$: $\mathbf{Q}_x(j\omega) = \mathbf{W}_x^{\top}(-j\omega)\mathbf{W}_x(j\omega)$ and $\mathbf{R}_u(j\omega) = \mathbf{W}_u^{\top}(-j\omega)\mathbf{W}_u(j\omega)$ where

$$\mathbf{z}_x(s) = \mathbf{W}_x(s)\mathbf{x}(s) \begin{cases} \dot{\mathbf{x}}_{xf} & = \mathbf{A}_{xf}\mathbf{x}_{xf} + \mathbf{B}_{xf}\mathbf{x} \\ \mathbf{z}_x & = \mathbf{C}_{xf}\mathbf{x}_{xf} + \mathbf{D}_{xf}\mathbf{x} \end{cases},$$

$$\mathbf{z}_u(s) = \mathbf{W}_u(s)\mathbf{u}(s) \begin{cases} \dot{\mathbf{x}}_{uf} & = \mathbf{A}_{uf}\mathbf{x}_{uf} + \mathbf{B}_{uf}\mathbf{u} \\ \mathbf{z}_u & = \mathbf{C}_{uf}\mathbf{x}_{uf} + \mathbf{D}_{uf}\mathbf{u} \end{cases}$$

Equation (24) can now be simplified as follows

$$\begin{aligned} \mathcal{J}_{rf} &= \frac{1}{4\pi}\int_{-\infty}^{\infty} [\mathbf{z}_x^{\top}(j\omega)\mathbf{z}_x(j\omega) + \mathbf{z}_u^{\top}(j\omega)\mathbf{z}_u(j\omega)]\mathrm{d}\omega \\ &= \frac{1}{2}\int_0^{\infty} (\mathbf{x}_{rf}^{\top}\mathbf{Q}_{rf}\mathbf{x}_{rf} + 2\mathbf{x}_{rf}^{\top}\mathbf{N}_{rf}\mathbf{u} + \mathbf{u}^{\top}\mathbf{R}_{rf}\mathbf{u})\,\mathrm{d}t \\ &= \frac{1}{2}\int_0^{\infty} [\mathbf{x}_{rf}^{\top}(\mathbf{Q}_{rf} - \mathbf{N}_{rf}\mathbf{R}_{rf}^{-1}\mathbf{N}_{rf}^{\top})\mathbf{x}_{rf} + \mathbf{u}'^{\top}\mathbf{R}_{rf}\mathbf{u}']\mathrm{d}t \end{aligned}$$

where $\mathbf{x}_{rf} = [\mathbf{x}^{\top}\ \mathbf{x}_{xf}^{\top}\ \mathbf{x}_{uf}^{\top}]^{\top}$, $\mathbf{u} = \mathbf{u}' - \mathbf{R}_{rf}^{-1}\mathbf{N}_{rf}^{\top}\mathbf{x}_{rf}$ and $\mathbf{Q}_{rf}$, $\mathbf{N}_{rf}$, and $\mathbf{R}_{rf}$ can be found via algebraic manipulation (see [24] and [26] for details). The frequency-weighted optimal state feedback matrix is then

$$\mathbf{K}_{rf} = \mathbf{R}_{rf}^{-1}(\mathbf{B}_{rf}^{\top}\mathbf{P}_{rf} + \mathbf{N}_{rf}^{\top}) = [\mathbf{K}_c\ \mathbf{K}_{xf}\ \mathbf{K}_{uf}]$$

where $\mathbf{P}_{rf}$ is found by solving a modified algebraic Riccati equation [28, 29].

A frequency-weighted optimal state estimator can also be derived [25, 30, 31]. To do so, the system disturbance, $\mathbf{d}$, and noise, $\mathbf{v}$, are taken to be the output of a set of differential equations

$$\mathbf{d}(s) = \mathbf{W}_d(s)\mathbf{d}'(s) \begin{cases} \dot{\mathbf{x}}_{df} & = \mathbf{A}_{df}\mathbf{x}_{df} + \mathbf{B}_{df}\mathbf{d}' \\ \mathbf{d} & = \mathbf{C}_{df}\mathbf{x}_{df} + \mathbf{D}_{df}\mathbf{d}' \end{cases},$$

$$\mathbf{v}(s) = \mathbf{W}_v(s)\mathbf{v}'(s) \begin{cases} \dot{\mathbf{x}}_{vf} & = \mathbf{A}_{vf}\mathbf{x}_{vf} + \mathbf{B}_{vf}\mathbf{v}' \\ \mathbf{v} & = \mathbf{C}_{vf}\mathbf{x}_{vf} + \mathbf{D}_{vf}\mathbf{v}' \end{cases}$$

where $\mathbf{d}'$ and $\mathbf{v}'$ are white noise sources [30]. The frequency weighted estimator weights are then $\mathbf{Q}_d(j\omega) = \mathbf{W}_d^{\top}(-j\omega)\mathbf{W}_d(j\omega)$ and $\mathbf{R}_v(j\omega) = \mathbf{W}_v^{\top}(-j\omega)\mathbf{W}_u(j\omega)$. In traditional LQG control, $\mathbf{d}$ and $\mathbf{v}$ are both zero mean white noise; here we are constructing disturbance and noise dynamics that change as a function of frequency.Constructing an optimal observer we have

$$\dot{\hat{\mathbf{x}}}_{ef} = \mathbf{A}_{ef}\hat{\mathbf{x}}_{ef} + \mathbf{B}_{ef}\mathbf{u} - \mathbf{K}_{ef}(\mathbf{C}_{ef}\hat{\mathbf{x}}_{ef} - \mathbf{y})$$

where $\hat{\mathbf{x}}_{ef}^{\top} = [\hat{\mathbf{x}}^{\top}\ \hat{\mathbf{x}}_{df}^{\top}\ \hat{\mathbf{x}}_{vf}^{\top}]$ and

$$\mathbf{K}_{ef} = \begin{bmatrix} \mathbf{K}_e \\ \mathbf{K}_{df} \\ \mathbf{K}_{vf} \end{bmatrix}$$

is found by solving a modified algebraic Riccati equation [28, 29]. $\mathbf{A}_{ef}$, $\mathbf{B}_{ef}$ and $\mathbf{C}_{ef}$ can be found by algebraic manipulation.

It follows then that the complete controller dynamics, that is the frequency-weighted optimal controller, can be written as (see equation at the bottom of the page).

5.2 Controller design via numerical optimisation

By adjusting the filters $\mathbf{W}_x(s)$, $\mathbf{W}_u(s)$, $\mathbf{W}_d(s)$, and $\mathbf{W}_v(s)$ the controller can be tuned to satisfy, for example, low and high-frequency gain criteria.In particular, a controller that is hybrid VSP/finite gain is sought, possessing VSP properties below ω_c, and finite-gain properties above ω_c. Rather than tuning the filters manually, a numerical optimisation

$$\begin{bmatrix} \dot{\hat{\mathbf{x}}} \\ \dot{\mathbf{x}}_{xf} \\ \dot{\mathbf{x}}_{uf} \\ \dot{\hat{\mathbf{x}}}_{df} \\ \dot{\hat{\mathbf{x}}}_{vf} \end{bmatrix} = \underbrace{\begin{bmatrix} (\mathbf{A} - \mathbf{K}_e\mathbf{C}_{yx} - \mathbf{B}_u\mathbf{K}_c) & -\mathbf{B}_u\mathbf{K}_{xf} & \mathbf{B}_u\mathbf{K}_{uf} & \mathbf{B}_d\mathbf{C}_{df} & -\mathbf{K}_e\mathbf{D}_{yv}\mathbf{C}_{vf} \\ \mathbf{B}_{xf} & \mathbf{A}_{xf} & \mathbf{0} & \mathbf{0} & \mathbf{0} \\ -\mathbf{B}_{uf}\mathbf{K}_c & -\mathbf{B}_{uf}\mathbf{K}_{xf} & (\mathbf{A}_{uf} - \mathbf{B}_{uf}\mathbf{K}_{uf}) & \mathbf{0} & \mathbf{0} \\ -\mathbf{K}_{df}\mathbf{C}_{yx} & \mathbf{0} & \mathbf{0} & \mathbf{A}_{df} & -\mathbf{K}_{df}\mathbf{D}_{yv} \\ -\mathbf{K}_{vf}\mathbf{C}_{yx} & \mathbf{0} & \mathbf{0} & \mathbf{0} & (\mathbf{A}_{vf} - \mathbf{K}_{vf}\mathbf{D}_{yv}\mathbf{C}_{vf}) \end{bmatrix}}_{\bar{\mathbf{A}}_c}$$

$$\underbrace{\begin{bmatrix} \hat{\mathbf{x}} \\ \mathbf{x}_{xf} \\ \mathbf{x}_{uf} \\ \hat{\mathbf{x}}_{df} \\ \hat{\mathbf{x}}_{vf} \end{bmatrix}}_{\bar{\mathbf{x}}_c} + \underbrace{\begin{bmatrix} \mathbf{K}_e \\ \mathbf{0} \\ \mathbf{0} \\ \mathbf{K}_{df} \\ \mathbf{K}_{vf} \end{bmatrix}}_{\bar{\mathbf{B}}_c} \mathbf{y}$$

$$-\mathbf{u} = \underbrace{\begin{bmatrix} \mathbf{K}_c & \mathbf{K}_{xf} & \mathbf{K}_{uf} & \mathbf{0} & \mathbf{0} \end{bmatrix}}_{\bar{\mathbf{C}}_c} \begin{bmatrix} \hat{\mathbf{x}} \\ \mathbf{x}_{xf} \\ \mathbf{x}_{uf} \\ \hat{\mathbf{x}}_{df} \\ \hat{\mathbf{x}}_{vf} \end{bmatrix}$$

problem will be posed, and the optimiser will tune the controller while simultaneously ensuring it satisfies the hybrid VSP/finite-gain constraints.

The optimisation constraints are $\delta_2 > 0$, $\kappa_2 < \infty$, $\gamma_1\gamma_2 < 1$, that is the controller satisfies the hybrid passivity/finite gain stability theorem. The optimisation objective function will be minimisation of the closed-loop $\mathcal{H}_2$-norm, as presented in (23), where the frequency-weighted controller is used in place of the standard $\mathcal{H}_2$ controller in (22). Minimisation of the closed-loop $\mathcal{H}_2$-norm is reasonable in that the closed-loop system should behave optimally.

How the filters should be parameterised is an interesting problem. Consider the design of the state feedback gain matrix where $\mathbf{Q}_x(j\omega)$ and $\mathbf{R}_u(j\omega)$ must be parameterised. At low frequency the control system should perform very well enabling trajectory tracking, for example. Logically, $\mathbf{Q}_x(j\omega)$ should be large and $\mathbf{R}_u(j\omega)$ should be small (in a relative sense) at low frequency. At high frequency however, the bandwidth of the controller should be limited in order to avoid having high-frequency disturbances degrade system performance. Additionally, in order to satisfy the constraint $\gamma_1\gamma_2 < 1$, the controller is expected to have gain that subsides past ω_c. Naturally, $\mathbf{Q}_x(j\omega)$ should be small and $\mathbf{R}_u(j\omega)$ should be large (again, in a relative sense) at high frequency, and in particular above ω_c. If, then, $\mathbf{W}_x(j\omega)$ is a low-pass filter and $\mathbf{W}_u(j\omega)$ is a high-pass filter, the controller will have the aforementioned characteristics. Consider, then, the following $\mathbf{W}_x(j\omega)$ and $\mathbf{W}_u(j\omega)$ parameterisations

$$\mathbf{W}_{x_{(i,j)}}(s) = K_{x_{(i,j)}} \frac{\omega_{(i,j)}^2}{s^2 + 2\zeta_{(i,j)}\omega_{(i,j)}s + \omega_{(i,j)}^2},$$

$$\mathbf{W}_{u_{(i,j)}}(s) = K_{u_{(i,j)}} \frac{sT_{(i,j)} + 1}{sT_{(i,j)}\alpha_{(i,j)} + 1}$$

where $\mathbf{W}_{x_{(i,j)}}(s)$ is the $i-j$th element of $\mathbf{W}_x(s)$ and $\mathbf{W}_{u_{(i,j)}}(s)$ is the $i-j$th element of $\mathbf{W}_u(s)$. Each $\mathbf{W}_{x_{(i,j)}}(s)$ transfer function is a low-pass filter with gain $K_{x_{(i,j)}}$, while each $\mathbf{W}_{u_{(i,j)}}(s)$ transfer function is a lead filter with gain $K_{u_{(i,j)}}$. Notice also that $\mathbf{W}_{x_{(i,j)}}(s)$ is strictly proper and rolls off at high frequency, thus $\mathbf{Q}_x(j\omega) \geq 0$ over all frequencies. The filter $\mathbf{W}_{u_{(i,j)}}(s)$ however has finite gain even as $\omega \to \infty$, thus $\mathbf{R}_u(j\omega) > 0$. In a numerical optimisation setting, $K_{x_{(i,j)}}$, $\zeta_{(i,j)}$, $\omega_{(i,j)}$, $K_{u_{(i,j)}}$, $T_{(i,j)}$, and $\alpha_{(i,j)}$ will be the design variables. With these filters, some additional constraints must be added; each filter parameter must be strictly positive and $0 < \alpha_{(i,j)} < 1$.

The matrices $\mathbf{Q}_d(j\omega) = \mathbf{W}_d^\top(-j\omega)\mathbf{W}_d(j\omega)$ and $\mathbf{R}_v(j\omega) = \mathbf{W}_v^\top(-j\omega)\mathbf{W}_u(j\omega)$ are parameterised in a similar manner. At high frequency, noise will significantly corrupt the available measurements. Thus, $\mathbf{W}_v(s)$ will be composed of lead filters representing low signal noise at low frequency, and significant signal noise at high frequency. External disturbances generally do not have very large magnitudes at high frequency. As such, $\mathbf{W}_d(s)$ will be composed of low-pass filters to capture this roll-off effect at high frequency. $\mathbf{W}_d(j\omega)$ (and hence $\mathbf{Q}_d(j\omega)$) could also be tuned to capture the presence of specific disturbances at specific frequencies [30]. Using this parameterisation, $\mathbf{Q}_d(j\omega) \geq 0$ and $\mathbf{R}_v(j\omega) > 0$ [25].

Our numerical optimisation problem can now be summarised.

Design Variables: parameterisation of $\mathbf{W}_x(s)$, $\mathbf{W}_u(s)$, $\mathbf{W}_d(s)$, and $\mathbf{W}_v(s)$.
Constraints: $\delta_2 > 0$, $\kappa_2 < \infty$ and $\gamma_1\gamma_2 < 1$ and the filter parameters must be admissible.
Objective Function: minimise $\mathcal{J} = \sqrt{\text{tr } \mathbf{B}_{zw}^\top \mathbf{P}_{zw} \mathbf{B}_{zw}}$.

To solve our optimisation problem, the numerical algorithm employed will be a sequential quadratic programming (SQP) algorithm where constraints are enforced via Lagrange multipliers and derivative information is acquired via finite differencing [32].

6 Experimental implementation and results

6.1 Experimental apparatus

The control architecture discussed in this paper will be implemented on the two-link flexible manipulator test-bed shown in Fig. 3. The apparatus is manufactured by Quanser Consulting Inc. The links are made of steel; the first link is 210.00 mm long, 1.27 mm thick, and 76.20 mm high, while the second link is 210.00 mm long, 0.89 mm thick, and 38.1 mm high. Affixed to the base of each link is a strain gauge, while a digital encoder is mounted to the output shaft of each motor. The encoders provide $\boldsymbol{\theta} = [\theta_1 \ \theta_2]^\top$, the base joint angle θ_1 and the elbow joint angle θ_2, and the strain gauges are used to determine the deflection in each link. Readers interested in other specific details of the apparatus are referred to [33]. Since $\boldsymbol{\theta}$ is directly measured, proportional control can be implemented with ease; the proportional control gain will be set to $\mathbf{K}_p = \text{diag}\{40, 40\}$ N · m/rad. The velocity $\dot{\boldsymbol{\theta}}$ is not directly measured, and will be acquired by filtering $\boldsymbol{\theta}$ with $\mathbf{F}(s)$ (as shown in (3)) thus destroying the passive nature of the nominal plant.

It is worth noting that a passivity violation will occur regardless of the derivative filter's bandwidth. However, in

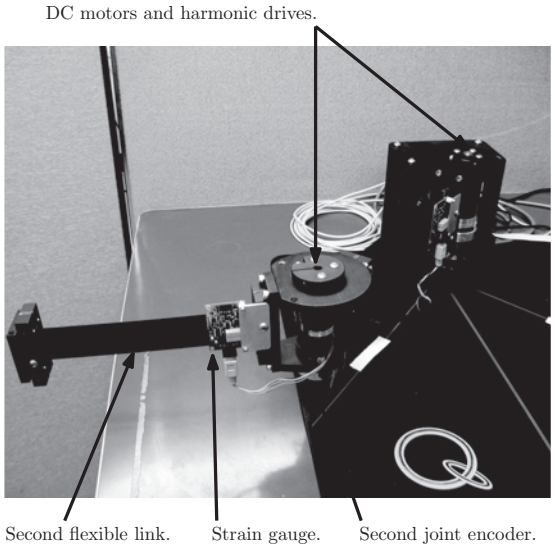

Fig. 3 *Two-link flexible robot experiment manufactured by Quanser Inc*

doi: 10.1049/iet-cta.2012.0459

some instances that passivity violation may occur at lower frequencies. Ideally the derivative filter's bandwidth is high enough that the derivative filter dynamics and the plant dynamics (i.e. the structural dynamics of the manipulator) do not interact. In this situation, the passivity violation would occur at high frequency. In practice, the derivative filter's bandwidth is reduced in order to avoid the excitation of high-frequency measurement noise. As such, the derivative filter dynamics will interact with the plant dynamics. In this case, the passivity violation will occur at a lower frequency.

6.2 Controller optimisation results

Rather than controlling the two-link manipulator system with one hybrid VSP/finite gain controller, two LTI hybrid VSP/finite gain controllers will be used within the scheduling architecture of Section 4. The first controller will be designed about set-point one corresponding to $\boldsymbol{\theta}_1 = [\theta_{1,1}\ \theta_{1,2}] = [0\ 0]^\top$ rad, and the second about $\boldsymbol{\theta}_2 = [\theta_{2,1}\ \theta_{2,2}] = [\pi/4\ \pi/4]^\top$ rad.

The two-link system is non-linear; to use the optimisation scheme proposed in Section 5.2, the dynamics are linearised about a specific joint configuration, $\boldsymbol{\theta}_\mathrm{i}$. Given the ideal plant along with some assumed sensor and actuator dynamics based on the test-bed discussed in Section 6.1, the critical frequency and high frequency gain, ω_c and γ_1, about set point $\boldsymbol{\theta}_\mathrm{i}$ can be estimated; in particular, $\omega_\mathrm{c} = 250\,\mathrm{rad/s}$, while $\gamma_1 = 0.2\,\mathrm{rad}/(\mathrm{N}\cdot\mathrm{m}\cdot\mathrm{s})$ for each set point. Because the true system is non-linear, it is assumed that the true non-linear high-frequency gain is close in magnitude to the estimated value γ_1. Note that there is uncertainty associated with ω_c and γ_1 because there is uncertainty associated with the additional dynamics that violate passivity. However, the values of ω_c and γ_1 are chosen in a slightly conservative way; the passivity violation may occur at a higher frequency, and γ_1 may in fact be smaller. However, attempting to determine ω_c and γ_1 more accurately would contradict the motivation behind the use of the hybrid passivity/finite gain stability theorem. The hybrid passivity/finite gain stability theorem is being used because below ω_c the plant has passive characteristics, and above ω_c the plant has finite gain.

Recall from Section 2.1 that the ideal system has a passive map from $\boldsymbol{\tau}$ to $\dot{\boldsymbol{\theta}}$. This map remains passive regardless of the number of flexible modes modelled, or the mass distribution of the manipulator, which is why passivity-based control is robust. When a passivity violation has been experienced and the hybrid passivity/finite gain framework is employed, at low frequency we enjoy these robustness properties because the plant remains passive and the controller is VSP in this range, and at high frequency we also enjoy robustness provided the gain of the plant remains below the critical value of γ_1, which is conservatively chosen.

The optimisation formulation of Section 5.2 is used to design two controllers. In Fig. 4, is the frequency response of the controller optimally designed about set-point one. The maximum singular value is $\bar{\sigma}(\mathbf{G}(j\omega))$ and the minimum Hermitian part is $\frac{1}{2}\underline{\lambda}[\mathbf{G}^\top(-j\omega) + \mathbf{G}(j\omega)]$, where $\mathbf{G}(j\omega)$ is the transfer matrix of controller one. Also included in Fig. 4 is the frequency response of a traditional $\mathcal{H}_2$ controller designed about set-point one where $\bar{\mathbf{Q}}_x = \mathbf{Q}_x(j0)$ and $\bar{\mathbf{R}}_u = \mathbf{R}_u(j0)$ are used to design the state feedback matrices, and $\bar{\mathbf{Q}}_d = \mathbf{Q}_d(j0)$ and $\bar{\mathbf{R}}_v = \mathbf{R}_v(j0)$ are used to calculate the observer gain matrices. Compared with the hybrid VSP/finite controller, the $\mathcal{H}_2$ controller has greater gain at high frequency, and with the linearised plant model do not satisfy the hybrid passivity/finite gain stability theorem.

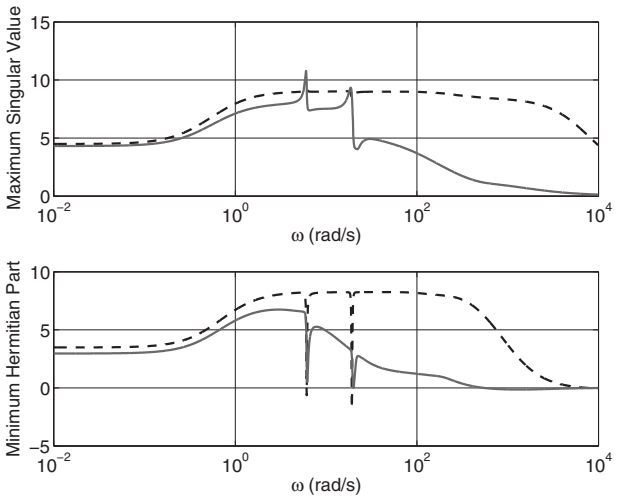

Fig. 4 *Hybrid VSP/finite gain (solid line) and traditional $\mathcal{H}_2$ (dashed line) controllers designed about set-point one*

6.3 Experimental results

The hybrid VSP/finite gain controllers designed using the optimisation formulation of Section 5.2 have been used within the scheduling architecture of Section 4 to control the two-link manipulator discussed in Section 6.1 (shown in Fig. 3).

The manipulator is to follow a desired trajectory starting at $\boldsymbol{\theta}_1$, moving to $\boldsymbol{\theta}_2$, then moving back to $\boldsymbol{\theta}_1$. The desired trajectory between set-points is

$$\boldsymbol{\theta}_d(t) = \left[10\left(\frac{t}{t_\mathrm{f}}\right)^3 - 15\left(\frac{t}{t_\mathrm{f}}\right)^4 + 6\left(\frac{t}{t_\mathrm{f}}\right)^5\right](\boldsymbol{\theta}_\mathrm{f} - \boldsymbol{\theta}_\mathrm{i}) + \boldsymbol{\theta}_\mathrm{i}$$

where t_f is 2 s, $\boldsymbol{\theta}_\mathrm{f}$ is the final angular position, and $\boldsymbol{\theta}_\mathrm{i}$ is the initial angular position. Between manoeuvres there is a 2 s dwell. It is worth noting that closed-loop stability of the system does not hinge on the trajectory chosen, nor on any sort of coupled motion of the two links. Although the trajectory is not all that challenging for a rigid manipulator, when the manipulator is flexible there is significant structure/controller interaction. Additionally, this trajectory uses up a significant portion of the torque capability of the motors. Should a more aggressive manoeuvre be considered, saturation would occur, which should be avoided.

Because two controllers are used within the scheduling architecture, there are two scheduling signals, s_1 and s_2. For simplicity, both scheduling signals will be linear functions of time, as shown in Fig. 5. Scheduling in this fashion is equivalent to scheduling in terms of the assumed trajectory of the manipulator. Because the scheduling signals are a function of time, the overall gain-scheduled controller is linear time-varying.

Recall the overall gain-scheduled controller maintains its hybrid VSP/finite-gain property as long as one scheduling signal is active at all times, and $s_i \in L_{2e} \cap L_\infty$. As such, robust L_2-stability of the closed-loop system is assured via the hybrid passivity/finite-gain stability theorem. Even if the

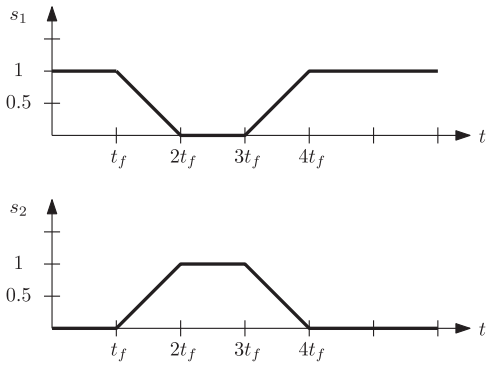

Fig. 5 *Scheduling signal profiles ($t_f = 2$ s)*

manipulator deviates from the desired trajectory because of disturbances, the gain-scheduled controller sill maintains its hybrid VSP/finite gain property, and the controller is assured to yield L_2-stability. Admittedly, the performance may suffer if the manipulator trajectory deviates from the desired trajectory.

Fig. 6 shows the response of the system controlled in two ways: the system is controlled by controller one only (ie no scheduling), and the system is controlled by both controllers and scheduled appropriately. Fig. 7 presents the error of each control scheme, while Table 1 presents the rms errors. Note the increase in performance when scheduling is used. In particular, in Figs. 6 and 7 one can clearly see a small vibration in θ_2 at set-point two that is not suppressed immediately. When scheduling is used, there is no vibration in θ_2 at set-point two. An explanation for this is simple: controller two is used in the scheduling scheme, and is fully active when the manipulator is at set-point two. Without scheduling, only controller one is used, and controller one is not optimally designed about set-point two, hence performance is degraded when the manipulator is away from set-point one.

We attempted to control the two-link system using the traditional $\mathcal{H}_2$ controllers. We found that the closed-loop was actually unstable when these controllers were used, which is why we do not present any trajectory or error plots. The reason the closed-loop is unstable is the gain of the traditional $\mathcal{H}_2$ controllers is very large at high frequency.

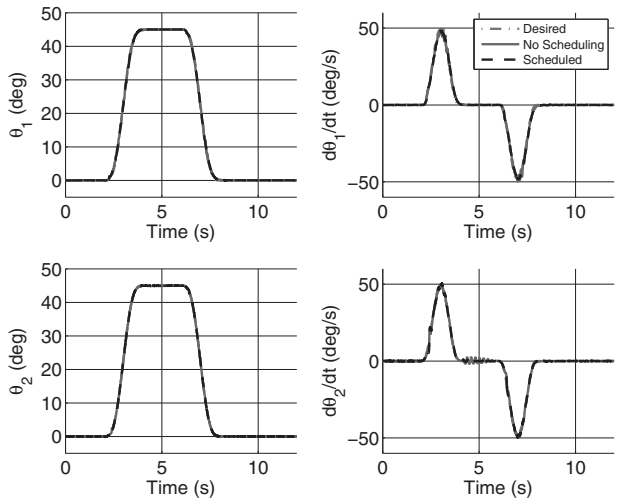

Fig. 6 *System response using hybrid VSP/finite-gain control and gain-scheduled hybrid control*

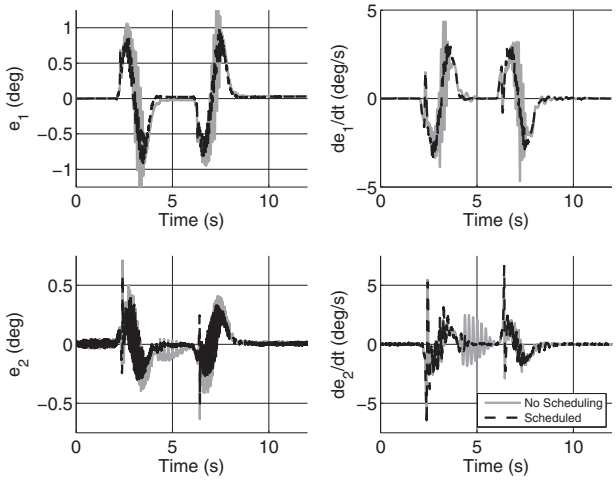

Fig. 7 *Position and velocity errors*

Table 1 Position and velocity rms errors

	θ_2 rms error (rad)	θ_2 rms error (rad)	$\dot{\theta}_1$ rms error (rad/s)	$\dot{\theta}_2$ rms error (rad/s)
Unscheduled	6.0×10^{-3}	2.2×10^{-3}	1.9×10^{-2}	1.6×10^{-2}
Scheduled	4.9×10^{-3}	1.6×10^{-3}	1.8×10^{-2}	1.6×10^{-2}

During operation high frequency noise and unmodelled dynamics are excited leading to instability. Comparatively, the hybrid VSP/finite gain controllers are forced to roll off to satisfy the hybrid passivity/finite-gain stability theorem. Note that the $\mathcal{H}_2$ controllers were not able to stabilise the system for the particular controller gains and derivative filter used. If more effort is made (i.e. tuning the controller further, tuning the derivative filter, modelling the plant more accurately, etc.) the $\mathcal{H}_2$ controllers do indeed work. However, it is interesting to note that the hybrid VSP/finite gain controllers (i.e. both the set-point one controller alone and the gain-scheduled controller) are able to stabilise and control the closed-loop system without such additional tuning.

7 Closing remarks

This paper considers closed-loop stability and controller design within the hybrid passive/finite-gain systems framework. Motivation is derived from the fact that nominally passive systems often have their passive I–O map destroyed in practice. In particular, the passive nature of a generic flexible robotic manipulator is discussed, as is a passivity violation induced by rate filters used to estimate the joint velocities of the manipulator.With a clear motivation, hybrid passive/finite gain systems and their stability in feedback are discussed. In particular, the VSP and finite gain parameters associated with LTI MIMO hybrid VSP/finite-gain systems are defined in terms of the Hermitian part and singular values of the system transfer matrix. The scheduling of hybrid VSP/finite-gain systems is considered as well, and it is shown that a set of hybrid VSP/finite-gain subsystems (which, in practice are often controllers) scheduled in an appropriate manner possesses properties that are hybrid VSP/finite gain. Controller design using a frequency-weighted optimal control formulation is also presented. Control of an experimental apparatus, a

doi: 10.1049/iet-cta.2012.0459

two-link flexible manipulator, successfully demonstrates practical application of the controller design formulation. Although the controller designed about one set-point performs well on its own, better closed-loop performance is attained while using two controllers (each optimal about a different set-point) scheduled appropriately.To summarise, the novel contributions of this work are:

1. Calculating the hybrid passivity and finite gain parameters δ, ϵ, and γ in an LTI MIMO context.
2. Showing that a gain-scheduled controller composed of hybrid VSP/finite gain subsystems has hybrid VSP/finite gain properties.
3. Using a frequency weighted optimal control formulation in conjunction with a numerical optimisation algorithm to design hybrid VSP/finite gain controllers.
4. Experimentally validating the controller design and scheduling schemes presented.

8 References

1 Anderson, B.D.O., Vongpanitlerd, S.: 'Network analysis and synthesis', (Englewood Cliffs, NJ: Prentice–Hal, 1973)
2 Desoer, C.A., Vidyasagar, M.: 'Feedback systems: input-output properties' (Academic Press, New York, 1975)
3 Ortega, R., Loria, A., Nicklasson, P.J., Sira-Ramirez, H.: 'Passivity-based control of Euler–Lagrange systems' (Springer, London, 1998)
4 Brogliato, B., Lozano, R., Maschke, B., Egeland, O.: 'Dissipative systems analysis and control: theory and applications' (Springer, London, 2nd edn., 2007)
5 Gao, Y.: 'Passive control for continuous singular systems with nonlinear perturbations', *IET Control Theory Appl.* 2010, **4**, (11), pp. 2554–2564
6 Wang, Y.: 'Passivity-based formation control of autonomous underwater vehicles', *IET Control Theory Appl.*, 2012, **6**, (4), pp. 518–525
7 Muhammad, S.: 'Passivity-based control applied to the dynamic positioning of ships', *IET Control Theory Appl.*, 2012, **6**, (5), pp. 680–688
8 Forbes, J.R., Damaren, C.J.: 'A hybrid passivity and finite gain stability theorem: stability and control of systems possessing passivity violations', *IET Control Theory Appl.*, 2010, **4**, (9), pp. 1795–1806
9 Forbes, J.R., Damaren, C.J.: 'Single-link flexible manipulator control accommodating passivity violations: theory and experiments', *IEEE Trans. Control Syst. Technol.*, 2012, **20**, (3), pp. 652–662
10 Griggs, W.M., Anderson, B.D., Lanzon, A.: 'A 'mixed' small gain and passivity theorem in the frequency domain', *Syst. Control Lett.*, 2007, **56**, (9–10), pp. 596–602
11 Griggs, W.M., Anderson, B.D., Lanzon, A., Rotkowitz, M.C.: 'Interconnections of nonlinear systems with 'mixed' small gain and passivity properties and associated input–output stability results', *Syst. Control Lett.*, 2009, **58**, (4), pp. 289–295
12 Iwasaki, T., Hara, S., Yamauchi, H.: 'Dynamical systems design from a control perspective: finite frequency positive-realness approach', *IEEE Trans. Autom. Control*, 2003, **48**, (8), pp. 1337–1354
13 Balas, M.J.: 'Active control of flexible systems', *J. Optim. Theory Appl.*, 1978, **25**, (3), pp. 415–436
14 Balas, M.J.: 'Feedback control of flexible systems', *IEEE Trans. Autom. Control*, 1978, **23**, pp. 673–679
15 Junkins, J.L., Kim, Y.: 'Introduction to dynamics and control of flexible structures' (American Institute of Aeronautics and Astronautics, Washington, DC, 1993)
16 Kelkar, A., Joshi, S.: 'Control of nonlinear multibody flexible space structures' (Springer, London, 1996)
17 Apkarian, P., Adams, R., 'Advanced gain-scheduling techniques for uncertain systems', *IEEE Trans. Control Syst. Technol.*, 1997, **6**, (1), pp. 21–32
18 Gevarter, W.B.: 'Basic relations for control of flexible vehicles', *AIAA J.*, 1970, **8**, (4), pp. 666–671
19 Damaren, C.J.: 'Gain-scheduled SPR controllers for nonlinear flexible systems', *J. Dyn. Syst., Meas. Control*, 1996, **118**, (4), pp. 698–703
20 Forbes, J.R., Damaren, C.J.: 'Design of gain-scheduled strictly positive real controllers using numerical optimization for flexible robotic systems', *J. Dyn. Syst. Meas., Control*, 2010, **132**, (3), p. 034503
21 Vidyasagar, M.: 'Nonlinear systems analysis' (Prentice–Hall, Englewood Cliffs, NJ, 2nd edn., 1993)
22 Moylan, P.J., Hill, D.J.: 'Stability criteria for large-scale systems', *IEEE Trans. Autom. Control*, 1978, **23**, (2), pp. 143–149
23 Green, M., Limebeer, D.J.N.: 'Linear robust control', (Prentice-Hall, Upper Saddle River, NJ, 1995)
24 Gupta, N.K.: 'Frequency-shaped cost functionals: extension of linear-quadratic-Gaussian design methods', *J. Guid. Control, Dyn.*, 1980, **3**, (6), pp. 592–535
25 Gupta, N.K.: 'Frequency-shaped penalty functions for robust control design'. Proc. American Control Conference, Arlington VA, 14–16 June, 1982, WP2-3:00, 1982
26 Imai, H., Kobayakawa, M.: 'Disturbance attenuation by a frequency-shaped linear-quadratic-regulator method', *J. Guid. Control, Dyn.*, 1986, **9**, (4), pp. 397–402
27 Anderson, B.D.O., Mingori, D.L.: 'Use of frequency dependence in linear quadratic control problems to frequency-shape robustness', *J. Guid. Control Dyn.*, 1985, **8**, (3), pp. 397–401
28 Friedland, B.: 'Control system design: an introduction to state-space methods' (McGraw-Hill Book Company, New York, 1985)
29 Bryson, A.E., Ho, Y.-C.: 'Applied optimal control' (Hemisphere Publishing, Washington, DC, 1975)
30 Gupta, N.K. 'Robust control/estimator design by frequency-shaped cost functionals'. Proc. Conf. Decision and Control, Dan Diego CA, 16–18 December, 1981, FA7-10:15, 1981
31 Anderson, B.D.O., Moore, J.B., Mingori, D.L.: 'Relations between frequency-dependent control and state weighting in LQG problems', *Opt. Control Appl. Methods*, 1987, **8**, (27), pp. 109–127
32 Nocedal, J., Wright, S.J.: 'Numerical optimization' (Springer, London, 2nd edn., 2000)
33 Quanser Consulting Inc., '2-DOF serial flexible link robot reference manual', 2010, Document Number: 763, Revision 1